AIAA JOURNAL
Vol. 48, No. 1, January 2010

Mixed-Variable Optimization Strategy Employing Multifidelity Simulation and Surrogate Models

Gulshan Singh* and Ramana V. Grandhi†
Wright State University, Dayton, Ohio 45435

DOI: 10.2514/1.43469

A progressive simulation-based design optimization strategy is developed that can be applied to highly nonlinear impulse-type processes such as shot peening, laser peening, and bullet impacts on aircraft structural components. The design problems entail the use of multiple fidelities in simulation, time-consuming elastic–plastic analysis, and mixed types of optimization variables. An optimization strategy based on progressively increasing the complexity and fidelity is developed, along with suitable surrogate models. Multilevel fidelity models include axisymmetric, symmetric three-dimensional, and full-scale simulations to enable design optimization. The first two models are used to perform parametric studies and to localize the potential design space. This creates a reduced design space and an effective starting point for the subsequent optimization iterations, using the proposed modified particle swarm optimization for mixed variables. In the third step, the full-scale model is employed to find an optimum solution. The design methodology is demonstrated on laser peening of a structural component. Laser peening is a surface enhancement technique that induces compressive residual stresses at the peened surface by generating elastic–plastic deformation. These stresses improve the surface fatigue life. The parameters, pressure pulse and spot dimensions, impulse locations (all continuous), number of shots (integer), and location of shots (discrete) are the optimization variables with stress constraints.

I. Introduction

MULTIDISCIPLINARY optimization of structures subjected to high-speed impact processes is complex due to the nonlinear and transient nature of the finite element analysis (FEA). The simulations consist of elastic–plastic analysis with small time steps and large-scale finite element models for practical aircraft structures. The experiment-based design approaches traditionally used are cost prohibitive for parameter optimization. Therefore, a simulation-based design methodology is required. In this paper, a design methodology is developed for structures subjected to the shock-type loadings that occur in shot peening, laser peening, explosions, and bullet impacts. The optimization problem is also challenging due to the presence of the continuous and discrete design variables [1], a mixed-variable optimization (MVO) problem.

In the literature, depending upon the geometry, loads, and boundary conditions, multifidelity simulation and surrogate models are used to solve aircraft structural analysis problems. Livne and Navarro [2] used polynomial-based equivalent plate modeling techniques for wing structure analysis. This work demonstrated that 2-D models can be used to approximate the nonlinear aeroelastic response of a wing box subjected to in-plane compressive forces. Robinson et al. [3] used physics-based and finite element models with parameter mapping on a wing design problem. This research proved that low- and high-fidelity models connected with parameter mapping can assist an optimization approach and save computational time. Chen et al. [4] employed multiple objective-oriented surrogate models, each constructed for a local region and combined using boolean operations. This approach updates the surrogate models based on the preexisting surrogate model and the confidence interval on approximation. Glaz et al. [5] compared a weighted average of multiple surrogate models (design of experiments, polynomial response, kriging, and radial basis neural network) with each individual surrogate model and demonstrated the advantage of the weighted-average surrogate [6,7]. Although these techniques are effective, they may not be the best options for impulse-type mixed-variable problems. In this research, a progressive mixed-variable optimization strategy is developed. This proposed strategy combines low- and high-fidelity simulations [2,3] and their respective surrogate models [4,5] and a mixed-variable strategy [1] to solve impulse-type problems.

The basis of the proposed mixed-variable optimization strategy is that, depending upon the problem information and assumptions, multiple simulation models can be developed to approximate the impulse response. Multiple impulses may be required in a process, but the effects of a single impulse at a location can be determined using a single axisymmetric model to address a large-scale problem. However, assumptions in the model limit the number of variables that can be considered in the model. Similarly, in a symmetric 3-D model, the number of assumptions can be reduced, so that this model can incorporate additional variables. Simulation of an arbitrary structural component with many impulses at multiple locations requires an analysis model without symmetric assumptions. Typically, such models are computationally expensive but can consider most problem variables. These qualities of the models are used in developing the optimization strategy. The uniqueness of the proposed method is that it localizes the design space using 2-D and symmetric 3-D simulation and surrogate models and determines the optima using mixed-variable particle swarm optimization.

As shown in Fig. 1, the strategy involves a three-step hierarchical procedure. This strategy employs low-fidelity models (2-D and symmetric 3-D) in the first two steps to locate the design space that may contain the optimal solution. This is achieved by parametric studies and by solving optimization problems, which also assist in eliminating insensitive optimization parameters. These steps provide an effective starting point and significantly reduce the search space for the third step of the optimization procedure. The reduced design space requires fewer function evaluations in the subsequent optimization step. When employed together, these three steps reduce the number of the full 3-D model simulations.

Presented as Paper 5838 at the 12th AIAA/ISSMO Multidisciplinary Analysis and Optimization Conference, Victoria, British Columbia, Canada,, 9 October–9 December 2008; received 28 January 2009; revision received 28 July 2009; accepted for publication 8 September 2009.

*Graduate Research Assistant; singh.31@wright.edu (Corresponding Author). Student Member AIAA.
†Distinguished Professor. Fellow AIAA.

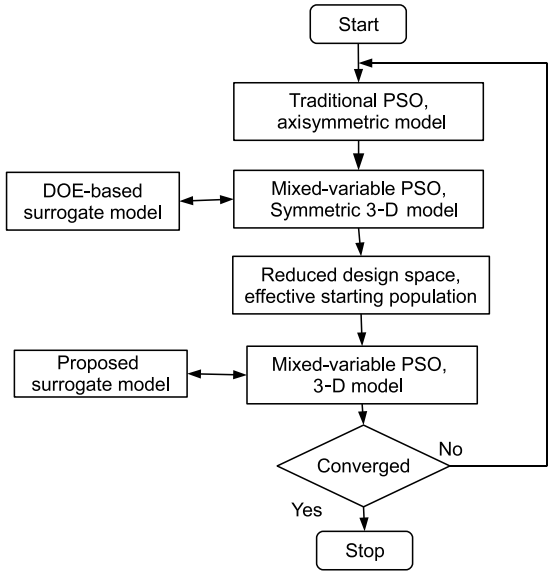

Fig. 1 Multifidelity optimization strategy.

The developed method is for impulse-type problems. There will always be an integer variable in such problems to represent the number of impulses. The lack of a generalized approach to handle mixed variables can be addressed by modifying standard particle swarm optimization (PSO) [8,9]. The modifications introduced are Latin hypercube sampling (LHS) based initial particle generation and a discrete variable handling technique.

II. Progressive Multifidelity Optimization Strategy

A. Optimization Technique: Particle Swarm Optimization

Population-based techniques are better suited to impulse-type problems due to the presence of mixed variables, the parallel processing advantage, and the no-function-gradients requirement. As compared with a genetic algorithm, another population-based technique, PSO has the advantages of a lower number of user input parameters, the use of historical information, and the ease of implementation. Therefore, PSO is selected as the optimization algorithm in each of the three steps of the strategy.

PSO, as proposed by Kennedy and Eberhart [8], uses a population-based approach that modifies the population from step to step based on a set of rules. In this set of rules, each individual (particle) uses its current fitness, its best fitness so far, the best fitness of all the individuals, and a communication structure to determine the movement of parameters. These parameters change over the course of iterations, and the particle population tends to converge and provide an optimum solution.

To better explore the design space and to handle discrete variables, two improvements are introduced into the traditional PSO procedure. In the first modification, the initial population is generated using LHS instead of random generation. This technique maintains randomness in the population and guarantees coverage of the entire design space. The covariance matrix required for LHS is obtained by assuming that all the parameters are independent and normally distributed. The second modification of the traditional PSO algorithm is illustrated using the following equation:

$$v_i^{k+1} = w_i v_i^k + c_{i1} r_{i1} \times (p\text{best}_i - s_i^k) + c_{i2} r_{i2} \times (g\text{best} - s_i^k) \quad (1)$$

where v_i^k is the velocity of the ith particle at iteration k, w_i is the weight function of the ith particle, c_{ij} is the weight coefficient of each term (jth) of the ith particle, r_{ij} is a random number between 0 and 1, s_i^k is the position of the ith particle at iteration k, $p\text{best}_i$ is the best value of the ith particle, and $g$best is the best value of the group. For c_{ij}, i depends upon the number of particles and j depends upon the number of terms in the velocity calculation [Eq. (1)]. The first term in the equation is called the inertia component of the PSO particles. In the second term $j = 1$, and in the third term $j = 2$. The term $j = 1$ guides the social behavior, whereas the term $j = 2$ dictates the cognitive behavior of the PSO particles.

In impulse-type problems, a typical integer variable is the number of impulses at the same location. A minor alteration in the random numbers r_{ij} of the velocity calculation [Eq. (1)] can help manage the integer variables. Because of the spacing and range of the integer variable, there are only a limited number of possibilities. Based on the random numbers, one possibility is selected. For example, if there are two possibilities for an integer variable, below or equal to 0.5 indicates the first possibility whereas above 0.5 indicates to the second. If there are three possibilities, the threshold will be 0.33 instead of 0.5; if four possibilities, then it will be 0.25. This modification allows both continuous and integer variables to be used in the procedure with no inconsistency. Because there is not an in-built termination criterion for PSO, depending upon the objective function requirements and available resources, the maximum number of function evaluations terminates the optimization:

$$\begin{aligned}
v_i^{k+1} &= w_i v_i^k + c_{i1} r_{i1} (p\text{best}_i - s_i^k) + c_{i2} r_{i2} (g\text{best} - s_i^k) \\
&\quad + c_{i3} r_{i3} (s_i^k - m\text{best}_i) \\
&= 0.5 \times (1) + 1 \times r_{i1}(2-1) + 1 \times r_{i2}(3-1) + 1 \times r_{i3}(1-2) \\
&= 0.5 + 1 \times \{0.0, 0.5, 1.0\} \times (2-1) + 1 \times r_{i2}(3-1) \\
&\quad + 1 \times r_{i3}(1-2) \\
&= 0.5 + 1 \times 0.5 \times (1) + 1 \times r_{i2}(2) + 1 \times r_{i3}(-1) \\
&= 0.5 + 0.5 + 1 \times \{0.0, 0.25, 0.50, 0.75, 1.0\} \times (2) \\
&\quad + 1 \times r_{i3}(-1) \\
&= 0.5 + 0.5 + 1 \times 0.25 \times (2) + 1 \times r_{i3}(-1) \\
&= 0.5 + 0.5 + 0.5 + 0.5 \times (-1) \\
&= 0.5 + 0.5 + 0.5 - 0.5 \\
v_i^{k+1} &= 1
\end{aligned}$$

The integer handling technique is explained using an example. It is assumed that, at iteration k, $w_i = 0.5$, $v_i^k = 1$, $s_i^k = 1$, $p\text{best}_i = 2$, $g\text{best} = 3$, $m\text{best}_i = 2$, $c_{i1} = 1$, $c_{i2} = 1$, and $c_{i3} = 1$. These values are substituted in Eq. (1) and the velocity at iteration $k + 1$ is calculated. As shown in the example, three random numbers (r_{i1}, r_{i2}, and r_{i3}) are needed to calculate the velocity v_i^{k+1}. The random numbers are decided in the sequence of r_{i1}, r_{i2}, and then r_{i3}. There are three options for r_{i1}: 0.0, 0.5, and 1.0. These options will make the second terms 0.0, 0.5, and 1.0, respectively. Let us assume that a random number generation selected 0.5 out of three possibilities. Therefore, the second term is 0.5. Similarly, there are five options for r_{i2}. For r_{i2}, out of five possibilities, random number generation selected 0.25. This makes the third term 0.5. In the fourth term, the random number r_{i3} has only one option. The option is 0.5. The velocity v_i^{k+1} is 1. A similar procedure is used to handle integer variables.

B. Proposed Surrogate Model

A property of impulse-type problems is that the impulses are repeated. A surrogate model is developed for the 3-D model that uses this repetitiveness. This surrogate model is based on the characteristic of an impulse-type problem that each impulse has a certain set of parameters that define it. If two impulse locations on a structure are significantly apart from each other and the parameters defining these impulses are the same, then both impulses generate similar local effects. The proposed model exploits this quality of the impulse response. The major advantage of this idea is that it does not require simulation of all impulses at different locations to approximate the cumulative effect of all impulses.

For a traditional design of an experiment-based surrogate model, a certain number of simulations are performed. The results of these simulations are used to construct an approximation. This is not the

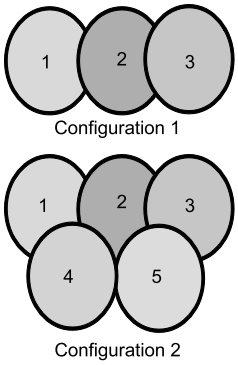

Fig. 2 Two possible layouts.

best approach for nonlinear impulse-type problems due to the computational cost of each simulation. In this surrogate model, instead of performing a complete simulation for each impulse, simulations for two or three impulses are performed to extract the effects of individual parameters. A three-impulse simulation requires less time as compared with a five-impulse simulation while still providing the information required to build a database for the surrogate model. Once all the individual parameters and interaction effects are extracted, they can be combined to approximate the performance for most configurations.

This concept is explained using two configurations. Figure 2a shows a three-impulse layout. The effects for this layout can be approximated using simulation of only two impulses, because the third impulse does not directly overlap with the first impulse. Similarly, Fig. 2b shows a five-impulse layout. Because the maximum number of directly interacting impulses is three, multiple three-impulse simulations can be used to approximate the resulting performance. After the database is generated, it can be used to approximate a solution for the required layout.

Although this surrogate model reduces the computational cost, it has two disadvantages. The first disadvantage is that it partially ignores the effects of impulse sequence. The second disadvantage is that, irrespective of the distance between the two impulses unless they overlap, the interaction effect is neglected. These drawbacks are not significant when compared with the advantages of the surrogate model. Moreover, because full simulations are performed after each optimization iteration convergence, the surrogate model serves as an intermediary interactive tool and the final analysis at the optimum is always conducted without making any of the aforementioned approximations.

C. Progressive Multifidelity Optimization Strategy Steps

This section presents the steps involved in the optimization strategy. Before starting the optimization procedure, various fidelity models (2-D, symmetric 3-D, and full-scale 3-D) need to be available. There are three steps in the optimization strategy:

1) The axisymmetric 2-D model is employed to determine parametric sensitivities and eliminate portions of the infeasible regions.

2) The symmetric 3-D model is employed to localize the design space and eliminate insensitive parameters. A typical design of experiments (DOE) based response surface model is used to assist in localizing the design space.

3) The full-scale 3-D model is employed to perform process optimization on the reduced design space. This step uses the surrogate model for impulse-type processes.

D. Advantages and Disadvantages of the Optimization Strategy

The proposed strategies have certain advantages and disadvantages. The first advantage is that the simpler models (axisymmetric) can often represent the physics of a problem more reliably. The proposed strategy uses this advantage by using 2-D and symmetric 3-D models. The second advantage is that the computational cost is lower than for the full 3-D models. The third advantage is that the stepwise process identifies infeasible regions without performing a full 3-D simulation. Thus, a disadvantage is that it is possible to lose some interaction effects among some parameters. This disadvantage can be avoided by performing parametric investigations before attempting the design optimization. Based on these investigations, the optimization strategy can be modified to accommodate the interaction effects.

The fourth advantage is that mixed variables are managed effectively without inconsistency. The fifth advantage is that the proposed surrogate model does not require simulation of all the impulses. An advantage of the proposed method, compared with a weighted average [5], is that a lower number of full-scale simulations are required for a global search of the design space. This is due to the use of lower-fidelity models.

Although the strategy is demonstrated here on an laser peening (LP) process optimization, the same strategy can be applied to many impulse-type problems, such as shot peening, bullet impacts, and shock loading of structures. To broaden the applicability of the strategy, additional extensive parametric investigations must be performed. The results of these parametric investigations can be used to determine the changes necessary to adopt the strategy for other problems. The new strategy can employ a different number of steps, number of simulation models, and types of simulation model.

III. Demonstration Problem: Laser Peening

A. Laser Peening Introduction

LP is a surface enhancement technique that uses the shock wave generation capability of lasers to induce favorable residual stresses on the peened surface. Engineering components such as turbine blades, aircraft lugs, and automobile connecting rods experience fatigue and fretting [10] loading. In many cases, these operating conditions generate tensile stresses on the surface, which initiate and propagate cracks, ultimately leading to failure. The LP-induced residual stresses mitigate the effect of tensile stress, improve the material response on the surface, and enhance fatigue strength [11–13]. Apart from LP, shot peening [14] and low plasticity burnishing are other surface enhancement techniques. Among the major advantages of LP, four important ones are the absence of contact during the peening process, the ability to peen complicated geometries, the higher depth of compressive stress, and the repeatability and controllability of the process. These LP qualities make it a potential solution for extending the fatigue life of aircraft components.

As shown in Fig. 3, for the confinement regime of LP, the component surface to be peened is prepared with a dual layer: the first layer consists of a material opaque to the laser beam and the second layer consists of a material transparent to the laser beam. After component surface preparation, the laser beam is fired to generate a pressure wave in the component. The properties of the pressure wave generated in the component are a function of the properties of the laser beam. Depending upon these properties, the pressure wave generates elastic–plastic deformation, resulting in residual stresses.

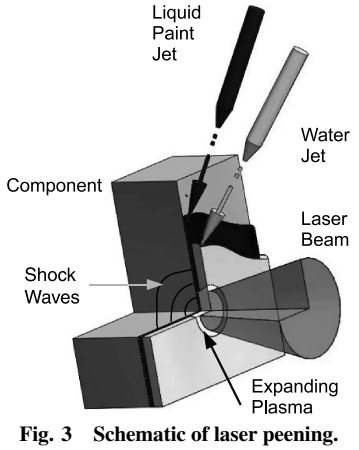

Fig. 3 Schematic of laser peening.

There are many parameters that can be controlled in LP. The pressure pulse magnitude and shape can vary between 3 and 10 GPa and 50 and 150 ns. The shape of the pressure pulse is also a function of the laser beam shape. The shape and size of the spot are other parameters that can be controlled. Many shapes of the shot are possible; however, circular and square are the most popular. The spot size can vary from 0.5 to 7 mm in diameter (or width). More than one laser shot is required for a typical application. Therefore, the location of the shots, the number of shots at the same location, and the layout of the shots play a significant role in optimization for engineering the resulting residual stress profile. The sequence of shots can also be a design parameter in LP.

The fatigue life of a peened component is a tradeoff between two opposing effects: the creation of compressive residual stresses on the surface, which tends to increase fatigue life, countered in part by the presence of tensile stresses, which tend to decrease fatigue life. Tensile stresses are present in the peened component to create static equilibrium with the compressive stress generated on the surface. Because of the lack of a direct mathematical relationship between LP parameters and compressive and tensile stress properties, LP cannot be easily implemented for maximum benefits. Typically, experience-based experimental processes have been used to obtain the optimal parameters for an application. For a typical job, the component is peened using a few (usually four) parameter settings. The engineer's experience is used to select these parameters so that experiments can be conducted. After peening, all these components are subjected to representative loading and, based on the improvement achieved in different components, the actual process parameters are selected. Depending upon the resources available, this process is repeated to refine the parameters. This is an expensive and time-consuming process; therefore, the proposed three-step optimization strategy is employed to optimize LP.

There are multiple challenges to implementing the three-step optimization strategy to optimize laser peening. The first challenge is to develop a simulation model that considers the required LP parameters. Preliminary simulation capabilities available in the literature [15–19] can consider a few LP parameters, such as pressure pulse properties (magnitude, duration, and shape), spot properties (shape and size), and number of shots at the same location. Although these variables can make a significant difference in the residual stress profile, current simulation capabilities are still not sufficient for optimization. A parametric model is required that can not only consider these variables but also the location of the shots, amount of overlap, and sequence of shots (mixed variables). The following sections present models available in the literature and develop a model to implement the optimization strategy.

B. Multiple Simulation Models of Laser Peening

Finite element simulations of a structure experiencing impulses can be performed using multiple models with respective assumptions. Depending upon the geometry and boundary conditions, response to an impulse can be modeled using axisymmetric, symmetric 3-D, or full-scale 3-D models.

1. Axisymmetric and Symmetric 3-D Models

To implement the proposed optimization strategy, axisymmetric (Fig. 4) and symmetric 3-D (Fig. 5) models developed by Singh et al. are used here [18,19]. The 2-D simulation is capable of modeling one shot of LP with a circular spot shape. The 2-D model can consider the pressure pulse magnitude and shape and the spot size. In addition to these design variables, the symmetric 3-D model can also consider the spot shape and number of shots.

2. Three-Dimensional Model

The 2- or 3-D simulations have applications in one or multiple shots at the same location. But a typical application may require 10–100 locations or shots on a large surface (50–500 mm); an FE model of such a system can be computationally prohibitive [20]. To investigate the effects of shots at more than one location, the different overlapping configurations, and the different sequences of shots, further improvements in the FE model are needed. A plate model is developed to investigate required parameters.

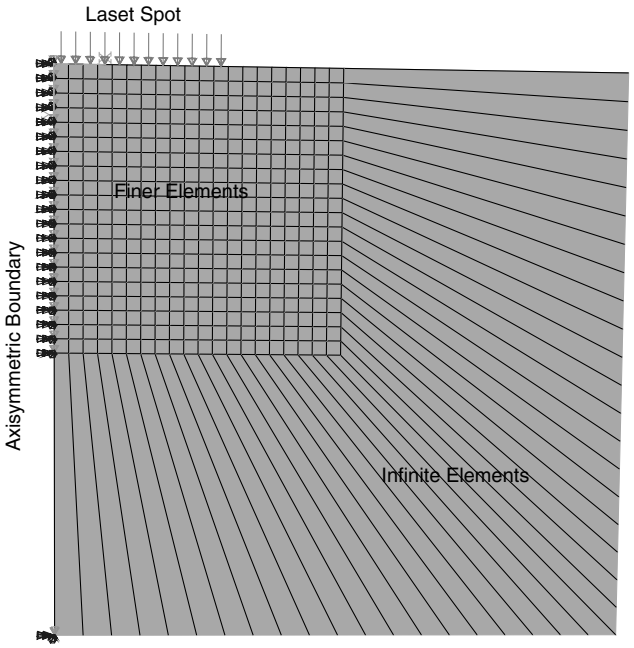

Fig. 4 Two-dimensional axisymmetric FEA model.

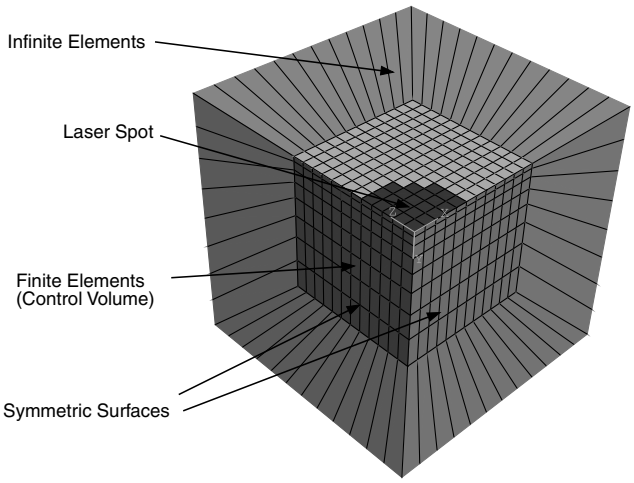

Fig. 5 Three-dimensional quarter FEA model.

The parameters of validated 3-D simulation methodology are used to develop the parametric plate model. Figure 6 shows the FE model of

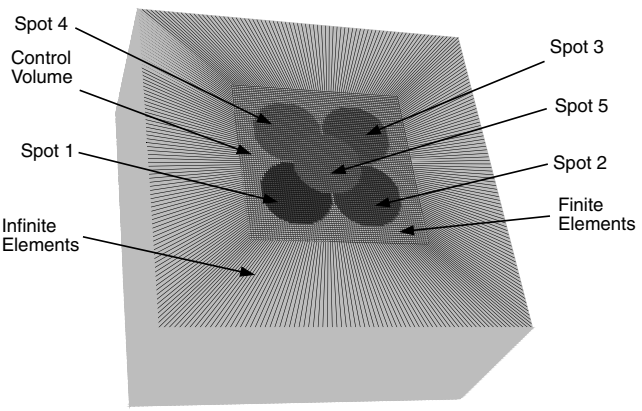

Fig. 6 FEA model of a plate with five shots.

the plate with a control volume size of $10 \times 10 \times 5$ (mm^3). As shown in the figure, infinite elements extend the plate by 5 mm on four sides and on the bottom of the plate. The figure shows five spot locations. These locations are variables to generate the desired overlapping configurations or totally separate spots. Apart from the parametric locations (or overlap), the model allows the designer to specify the spot size and shape, pressure pulse magnitudes, shapes and duration, number of shots at the same location, and sequence of shots.

IV. Optimization Formulation

A. Optimization Formulation: Mixed-Variable Optimization

For impulse-type loading, the objective of an optimization problem can be to minimize cost of the process, minimize or maximize damage, or maximize a performance function. The objective for LP is to maximize the compressive stress volume in the peened component. There are three constraints in the formulation. The first constraint is on the profile of the compressive stresses in the peened region. The constraint forces the compressive stresses at the surface to be maximum or within a certain range of maximum compressive stress magnitude. In mathematical terms, compressive stresses at depth d are constrained to be higher or within a certain range at depth $d + \Delta d$, where Δd is always positive. This constraint is included to mitigate the effects of the nonlinear behavior of the LP process. The nonlinear behavior is that a few parametric settings of the process produce reduced compressive stresses at the surface. This constraint avoids or reduces this behavior.

The second constraint is on the depth of the compressive stress at a selected point. This requires the depth of compressive stress to be more than 1 mm. The difference between the first and second constraints is that the first dictates the compressive profile in a region and the second dictates the presence of compressive stress at a prescribed depth. The third constraint controls the maximum magnitude of tensile stress. This constraint keeps the maximum magnitude of the tensile stresses below 150 MPa. The design variables are pressure pulse magnitude (p_i) and shape (t_{1i} and t_{1i}), spot shape (s_i) and size (r_i), location of shot (x_i and y_i), and number of shots at the same location (n_i). Here i indicates the ith shot. The lower and upper bounds for each variable are shown in the following formulation.

Maximize the compressive stress volume subject to compressive stress$(d) \geq$ compressive stress$(d + \Delta d)$, compressive stress depth ≥ 1.0 mm, and maximum tensile stress ≤ 150 MPa with the following variable bounds:

$$2.8 \leq p_i \leq 8.0 \text{ GPa}, \qquad 15.0 \leq t_{1i} \leq 50.0 \text{ ns}$$
$$50.0 \leq t_{2i} \leq 150.0 \text{ ns}, \qquad 0.5 \leq s_i \leq 1.0$$
$$2.0 \leq r_i \leq 3.0 \text{ mm}, \qquad 2.5 \leq x_i \leq 7.5 \text{ mm}$$
$$2.5 \leq y_i \leq 7.5 \text{ mm}, \qquad n_i = \{1, 2, 3\}$$

A traditional optimization based on the parametric plate model can consider this formulation and provide a solution. But a plate simulation of five shots at five locations requires 4 days of CPU time using eight dual core 2.6 GHz Opterons 8 GB RAM computers at the Ohio Supercomputing Center. A simulation for three shots at each of the five locations requires 12 days of CPU time. Because of the computational time issues, finding an optimal solution using the proposed progressive optimization strategy is more effective than the traditional optimization.

B. Implementation of the Optimization Strategy

The three models of LP required for the three-step optimization strategy, axisymmetric, symmetric 3-D, and the parametric plate, require approximately 20, 170, and 5760 min of CPU time, respectively. As a starting point of the three-step optimization strategy, parametric investigations [18] are performed to determine the effects of individual parameters. These investigations find a significant variation in parametric sensitivities with respect to performance metrics. In the first step of the strategy, three LP parameters (the pressure pulse magnitude and shape and the spot size) are optimized using a 2-D simulation. The second step considers four LP parameters (pressure pulse magnitude and duration, spot shape, and number of shots) and uses symmetric 3-D simulation. In the third step, four parameters (pressure pulse magnitude, spot location and size, number of shots at the same location) are considered.

C. Step 1: Optimization Using the 2-D Model

In this section, the first optimization step is implemented employing 2-D simulation. There are three LP parameters in the optimization: pressure magnitude (p), shot radius (r), and pressure pulse shape (t. As shown in Fig. 7, the pressure pulse shape is defined using two design variables, t_1 and t_2); as a result, there are a total of four design variables: p, r, t_1, and t_2. Based on the capabilities of the equipment, the peak pressure (p) range is 3.5–8.8 GPa, and the spot radius range is 2.0–3.0 mm. For pressure pulse shape, a sharp rise (peak in 3 ns) is preselected, and the rate of drop is determined by the variables t_1 and t_2. The ranges of the variables are such that these can generate any type of pulse between a sudden (lower limits) and slow (upper limits) pressure drop. The ranges of the two shape variables are 15–50 ns (t_1) and 90–150 ns (t_2). The optimization problem statement is given by the following.

Maximize the compressive stress volume subject to compressive stress$(d) \geq$ compressive stress$(d + \Delta d)$, compressive stress depth ≥ 1.0 mm, and maximum tensile stress ≤ 150 MPa with the following variable bounds:

$$3.5 \leq p \leq 8.8 \text{ GPa}$$
$$2.0 \leq r \leq 3.0 \text{ mm}$$
$$15.0 \leq t_1 \leq 50.0 \text{ ns}$$
$$90.0 \leq t_2 \leq 150.0 \text{ ns}$$

The number of particles and generations in the PSO is selected as 20. The values of c_{i1} and c_{i2} are taken as 1.7. The optimization results show that, to achieve the desired residual stress profile, a peak

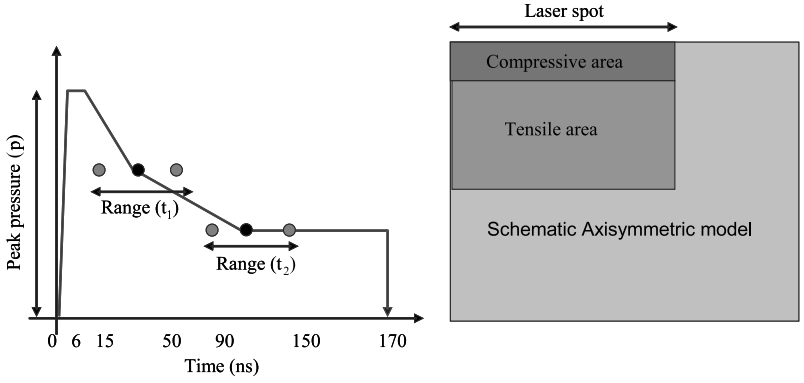

Fig. 7 Optimization Formulation.

pressure of 5.42 GPa, a spot radius of 2.1 mm, and pressure shape parameters of 17.0 and 150.0 ns are needed. The formulation is able to achieve the required depth and limit the maximum tensile stresses within the specified limit. The maximum tensile stress constraint is the active constraint at the optimum. It can be seen from the results that the low spot radius can keep the reduced compressive region at the center of the spot to within the limit. The first shape parameter (t_1) is near the lower bound of the variable range, and the second shape parameter (t_2) is at the upper bound of the variable range. This indicates a sharp drop, but a long pressure pulse is favored for the formulation.

D. Step 2: Optimization Using the Symmetric 3-D Model

In this section, the second step of the strategy is implemented, in which pressure pulse magnitude (p_i), number of shots (n), and laser shot shape (s_i) are considered as variables. The pressure pulse shape is taken from the previous step, and the pressure magnitude range is reduced for better exploration of the design space. This model obtains an effective starting point from the previous step but experiences computational cost challenges. A surrogate model is used to reduce the computational expense.

1. *Design of Experiment-Based Surrogate Model*

In many traditional methods, an approximation is constructed around a current point to obtain the next point. However, in the case of LP, only a limited number of simulations can be performed; therefore, a surrogate model that covers the entire move limits is required for each step. Traditionally, a model is required to predict an objective function and some constraints. However, in LP, the requirement is the residual stress values at all nodes. In the 3-D model, there are 44,800 nodes, and constructing the response surface for residual stresses of each node is necessary to calculate the performance metrics (objective and constraints).

To develop a surrogate model, a three-level full factorial design is considered. Simulations are performed to calculate residual stress values at all nodes in all designs of DOE. Because there are four variables, a total of (3^4=)81 simulations are performed. This setup provides the matrix [X] [Eq. (3)] and the response vector [Y] for each node to a construct response surface. But the interesting point to note is that all the nodes have the same [X] matrix because it is constructed for the same set of DOE parameters. However, the vector [Y] is different because it represents the residual stress values from simulations. For each node a surrogate model is assumed as shown in the following equation:

$$\hat{Y} = \hat{\beta}_0 + \hat{\beta}_1 f_1(x) + \cdots + \hat{\beta}_k f_k(x) + \epsilon \tag{2}$$

where β_i, $i = 0, 1, 2, \ldots, k$, are the unknown coefficients, ϵ is the residue in the regression model, and $f_i(x_j)$ are the functions of individual or combined x_i. The least-squares method is used to find unknown coefficients, and it yields

$$\hat{\beta} = (X^T X)^{-1} X^T Y \tag{3}$$

$$\hat{Y} = X\hat{\beta}, \qquad e = Y - \hat{Y} \tag{4}$$

Equations (3) and (4) are performed for each node. In the regression process, the most computationally intensive process is determining the inverse of the matrix ($X^T X$) in Eq. (3). This computational cost is much lower than that of the LP simulation. Based on these formulations, the coefficient $\hat{\beta}$ is calculated for all the nodes.

2. *Optimization Formulation and Results*

The variables are pressure pulse magnitude (p_i), spot shape (s_i), spot size (r), and the number of shots (n). The subscript i denotes the ith shot of the process. In the following formulation, the volume of the compressive region is the objective function. All the constraints and variable bounds for fatigue strength are shown as follows.

Maximize the compressive stress volume subject to compressive stress(d) $\geq$ compressive stress($d + \Delta d$), compressive stress depth $\geq$ 1.0 mm, and maximum tensile stress $\leq$ 150 MPa with the following variable bounds:

$$4.0 \leq p_i \leq 6.5 \text{ GPa}, \qquad 0.5 \leq s_i \leq 1.0$$
$$2.0 \leq r \leq 2.5 \text{ mm}, \qquad n_i = \{1, 2, 3\}$$

The results of the formulated problem show that two shots with pressure pulse magnitudes of 3.6 and 4.7 GPa, a radius of 2.28 mm, and shape parameters of 1.0 and 0.80 are the optimum. The pressure magnitude, radius, and shape variables are guided by the profile constraint. In this optimization, the stress profile constraint is an active constraint.

E. Methodology Validation

An assumption of the proposed optimization strategy is that a comparatively lower fidelity model (2-D) can provide a solution similar to that of higher fidelity models (3-D and plate). To validate this assumption, the problem formulated for the 2-D model is solved using both 2- and 3-D models. The same PSO parameters are used for both models. The termination criterion in both approaches is the maximum number of iterations. This is because a population-based technique can easily determine the potential region but can require a large number of iterations to find the converged optima.

The results from both models are shown in Table 1. The solutions in the table show that results from both models are similar. The table shows that the parameters, pressure magnitude ($p = 5.72$ and 5.58 GPa), and radius ($r = 2.49$ and 2.44 mm) are similar for both models. The pressure pulse shape parameters (t_1 and t_2) are different in both solutions. In the 2-D solution, t_1 is greater, and in the 3-D solution, t_2 is greater. These differences cancel each other out to some extent, bestowing similar results. A second problem is also solved using both models. The second problem is the same as the first problem, except that the constraint on the residual stress profile is removed. Table 1 shows that the results from both models are similar. The results of the second problem indicate that the pressure magnitude has a direct relationship with the compressive stress profile. The pressure magnitude is at its maximum possible value. The radius and shape are not at maximum to control the reduced compression at the center of the spot. This study shows that the 2-D simulation can be employed to save computational time and that the assumption made in the progressive optimization strategy is reasonable.

F. Step 3: Optimization Using the Parametric Plate Model

At this point, the first two steps of the optimization strategy have been implemented. The third step of the strategy is important because the model in this step considers the greatest number of variables of any model. For example, in LP, it is necessary to include the impulse location variables that can generate various overlapping configurations or layouts. To do that, it is necessary to use the parametric plate model. However, the required CPU time of 4 days for one simulation forces us to use the proposed surrogate model.

1. *Surrogate Model*

The parameters that define an LP shot are pressure pulse magnitude, shape and duration, spot shape and size, and amount of overlap. Two LP shots with the same parameters at two different locations generate similar local residual stress fields. Therefore, the proposed surrogate model can be applied to the LP problem. For the

Table 1 Results for methodology validation

Problem no.	Model used	p, GPa	r, mm	t_1, mm	t_2, ns
1	2-D	5.72	2.49	33.5	150.0
1	3-D	5.58	2.44	38.1	110.1
2	2-D	8.00	2.29	33.1	150.0
2	3-D	8.00	2.39	26.6	149.1

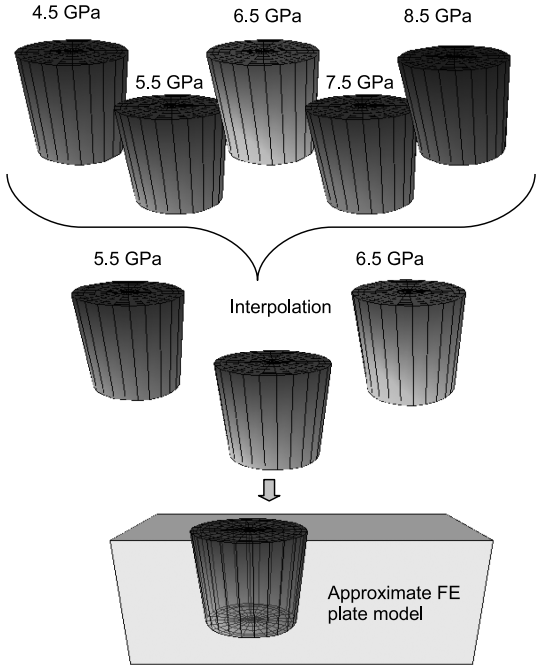

Fig. 8 Schematic of combining database information to obtain desired stress field.

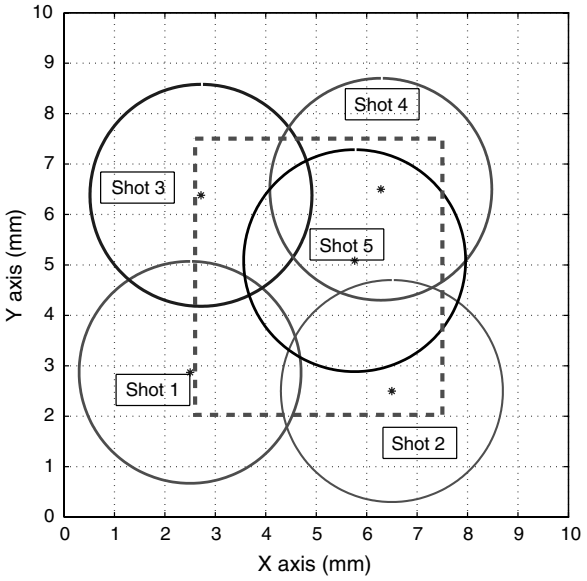

Fig. 9 Optimal layout of the peening process.

parametric plate, three-shot simulations are performed to extract the effects of individual parameters. Once the individual parameters and interaction effects are extracted, they can be combined to approximate the residual stress profile for most configurations.

An example of the surrogate model is shown in Fig. 8. This example is a schematic for only one variable (pressure magnitude). A database is available for 4.5, 5.5, 6.5, 7.5, and 8.5 GPa pressure magnitudes. The database for each magnitude contains residual stress values at the plate nodes. For example, to approximate the residual stress field for 6.0 GPa, the residual stress fields from 5.5 and 6.5 are used. The linear formulation to approximate the residual stress field is shown as follows:

$$R_{6.0} = \frac{6.0 - 5.5}{6.5 - 5.5} R_{5.5} + \frac{6.5 - 6.0}{6.5 - 5.5} R_{6.5} \tag{5}$$

where $R_{(p)}$ indicates the residual stress field at pressure p.

Equation (5) shows linear interpolation for one variable surrogate model. Similarly, a surrogate model can be developed for any number of variables. An example for two variables is pressure pulse magnitude (4.5, 5.5, 6.5, 7.5, and 8.5 GPa) and amount of overlap (0, 25, 50, 75, and 100%). In this example, a database is needed that can generate a five-shot residual stress profile for any combination of the pressure pulse magnitude and overlap. Different permutations and combinations of a three-shot sequence are used to generate the database.

To generate the residual stress field for five shots on different locations with a 20% overlap for the second through fifth shots and a 6.1 GPa pressure for all shots, the following process is used. The effects of the first shot are directly interpolated from the local residual stress fields of 5.5 and 6.5 GPa magnitudes. The second shot is interpolated from the local residual stress fields of 5.5 and 6.5 GPa pressure pulses and the local residual stress fields of the 0 and 25% overlap configurations. Similarly, the approximate residual stress field can be generated for any number of shots on the plate.

In this research, linear interpolation is used; however, depending upon the parametric investigations, this can be changed to higher-order interpolations. This approach does not use updates within the move limits. Just as with the surrogate model for the full 3-D model, this also provides the residual stress for all the nodes instead of a selected node. A limited number of five-shot simulations are needed to construct the database because the fifth shot is often located at the center of the plate, overlapping the previous four shots.

2. *Surrogate Model Validation*

The following investigations were performed to compare the estimates of the surrogate model with the FE simulations. Four random peening configurations are selected. FE analysis is performed to determine the compressive stress volume, depth, and maximum magnitude. The surrogate model is also used to determine these quantities. Here, p_i indicates the pressure magnitude of the ith shot, x_i indicates the x coordinate of the ith shot location, and y_i indicates the y coordinate of the ith shot location. The peening parameters in the first configuration are $p_1 = 4.1$, $p_2 = 5.3$, $p_3 = 4.6$, $p_4 = 5.1$, $p_5 = 3.9$, $x_1 = 3.6$, $x_2 = 5.8$, $x_3 = 2.9$, $x_4 = 5.6$, $x_5 = 4.1$, $y_1 = 3.8$, $y_2 = 3.2$, $y_3 = 6.4$, $y_4 = 5.8$, and $y_5 = 6.0$. The peening parameters in the second configuration are 4.7, 5.6, 4.3, 5.6, 4.7, 3.3, 6.4, 4.0, 5.6, 5.2, 3.1, 3.4, 5.7, 6.5, and 5.3. The peening parameters in the third configuration are 5.6, 4.2, 4.8, 4.6, 6.0, 2.6, 6.5, 4.3, 5.7, 5.0, 3.4, 2.9, 5.8, 5.9, and 4.6. The peening parameters in the fourth configuration are 5.5, 4.1, 5.7, 5.1, 5.1, 2.7, 6.4, 2.5, 6.4, 4.1, 4.4, 3.1, 5.9, 6.2, and 4.0. Table 2 shows the results from both approaches. The comparison shows that the approximation and the FE models do not match exactly. However, the surrogate model is able to capture the trends. The minimum errors in the compressive stress volume, depth, maximum magnitude, and tensile stress maximum magnitude are 21.2, 0.0, 8.7, and 0.06% and

Table 2 Comparison of results from surrogate and FEA models

	1		2		3		4	
	FEA	Approx..	FEA	Approx..	FEA	Approx..	FEA	Approx..
Compressive vol.	34.7	26.7	43.1	32.8	44.9	32.4	42.5	33.5
Max. compressive magnitude	−419.7	−479.8	−563.1	−612.1	−529.6	−623.6	−479.2	−398.3
Compressive depth	0.63	0.54	0.63	0.63	1.00	1.13	0.75	0.75
Max. tensile magnitude	77.1	93.8	97.6	98.5	84.8	85.3	110.0	97.0

Table 3 Results of optimization strategy

Shot No.	Pressure magnitude, GPa	Location x, mm	Location y, mm	Radius, mm	No. of shots
1	4.42	2.5	2.87	2.28	1
2	4.67	6.5	2.5	2.28	1
3	4.53	2.72	6.38	2.28	1
4	6.20	6.28	6.5	2.28	1
5	4.37	5.76	5.08	2.28	1

the maximum errors are 27.8, 14.3, 17.7, and 21.1%, respectively. Overall, the proposed surrogate model has potential use in iterative optimization. An important aspect to note is that the finite element analysis took 4 days of CPU time, whereas the surrogate model estimation took just 10_mins of CPU time. At the end of the surrogate-model-based optimization, complete finite element analysis is conducted for verifying the constraints' satisfaction. Based on the results, the next iteration of optimization is continued.

3. Optimization Formulation and Results

The optimization formulation and results of the third step are provided below. Similar to the results of the previous two steps, the results show that a lower pressure magnitude is favored because of the residual stress profile constraint. The spot layout is shown in Fig. 9. In this problem, the constraint on the residual stress profile and the maximum tensile stresses restrict the maximum compressive stress magnitude and the compressive stress volume.

Maximize the compressive stress volume subject to compressive stress$(d) \geq$ compressive stress$(d + \Delta d)$, compressive stress depth ≥ 1.0 mm, and maximum tensile stress ≤ 150 MPa with the following variable bounds:

$$2.5 \leq x_i \leq 7.5 \text{ mm}, \qquad 2.5 \leq y_i \leq 7.5 \text{ mm}$$
$$3.5 \leq p_i \leq 6.5 \text{ GPa}, \qquad n_i = \{1, 2, 3\}$$

The optimization results are given in Table 3. In addition to achieving the set objective and complying with the constraints, the optimization is able to find a layout that covers the region of interest. The region of interest is in between 2.0 to 7.5 on both (x and y) axes and is shown by a dotted line in Fig. 9. The results indicate that for the formulated problem, a pressure magnitude of approximately 4.5 GPa can achieve the objective. The magnitude of the 4th shot is different from the other shots at 6.2 GPa. A possible reason for this is that the fifth shot overlaps the fourth shot. Because of this overlap, the reduction of compressive stress at the center of the spot is negated by the subsequent shot. Another interesting result is that at all the locations the objective is achieved by using only one shot.

V. Conclusions

The optimization of structural components subjected to high-energy impulses could involve nonlinear elastic–plastic behavior, time-consuming finite element simulations, and mixed optimization variables. Because of these properties and problem-specific information, a traditional optimization method is not the best choice for these problems. To solve such problems, a progressive simulation-based mixed-variable optimization strategy is developed. The strategy begins with parametric investigations using lower-fidelity models to determine sensitive parameters and to localize the design space. In each step of the strategy, the design space is reduced and the parameters are eliminated with the goal of reaching an optimal solution. The strategy is demonstrated on a laser peening problem.

In general and from the demonstrated case, the following conclusions can be drawn:

1) For impulse-type problems, low-fidelity models can assist in reducing the infeasible design space and eliminating insensitive design variables.

2) The proposed surrogate model can assist in reducing the computational cost associated with optimizing impulse-type processes.

3) A systematic random number generation in PSO can handle mixed-variables without any inconsistency.

4) This design strategy can be applied to other impulse-type problems with mixed optimization variables.

5) In the laser peening process, pressure, pulse magnitude, number of shots, and spot layout are critical parameters.

Acknowledgments

This research work is funded by contract FA8650-04-D-3446, DO#25 from the Wright–Patterson Air Force Base, Ohio. The authors thank A.H. Clauer, D.F. Lahrman, and R.D. Tanaglia from LP Technologies, Inc., Columbus, Ohio, for their technical exchange.

References

[1] Olsen, G. N., and Vanderplaats, G. N., "Method for Nonlinear Optimization with Discrete Variables," *AIAA Journal*, Vol. 27, No. 11, 1989, pp. 1584–1589. doi:10.2514/3.10305

[2] Livne, E., and Navarro, I., "Nonlinear Equivalent Plate Modeling of Wing Box Structures," *Journal of Aircraft*, Vol. 36, No. 5, 1999, pp. 851–865. doi:10.2514/2.2519

[3] Robinson, T. D., Eldred, M. S., Willcox, K. E., and Haimes, R., "Surrogate-Based Optimization Using Multifidelity Models with Variable Parameterization and Corrected Space Mapping," *AIAA Journal*, Vol. 46, No. 11, 2008, pp. 2814–2822. doi:10.2514/1.36043

[4] Chen, S., Xiong, Y., and Chen, W., "Multiresponse and Multistage Metamodeling Approach for Design Optimiziation," *AIAA Journal*, Vol. 47, No. 1, 2009, pp. 206–218. doi:10.2514/1.38187

[5] Glaz, B., Goel, T., Liu, L., Friedmann, P., and Haftka, R., "Multiple-Surrogate Approach to Helicopter Rotor Blade Vibration Redcation," *AIAA Journal*, Vol. 47, No. 1, 2009, pp. 271–282. doi:10.2514/1.40291

[6] Kim, C., Wang, S., and Choi, K. K., "Efficient Response Surface Modeling by Using Moving Least-Squares Method and Sensitivity," *AIAA Journal*, Vol. 43, No. 11, 2005, pp. 2404–2411. doi:10.2514/1.12366

[7] Jin, R., Chen, W., and Simpson, T. W., "Comparative Studies of Metamodeling Techniques Under Multiple Criteria," *Structural and Multidisciplinary Optimization*, Vol. 23, No. 1, 2001, pp. 1–13. doi:10.1007/s00158-001-0160-4

[8] Kennedy, J., and Eberhart, R. C., "Particle Swarm Optimization," *Proceedings of the IEEE International Conference on Neural Networks*, IEEE Publications, Piscataway, NJ, 1995, pp. 1942–1948.

[9] Venter, G., and Sobieszczanski-Sobieski, J., "Multidisciplinary Optimization of a Transport Aircraft Wing Using Particle Swarm Optimization," *Structural and Multidisciplinary Optimization*, Vol. 26, Nos. 1/2, 2004, pp. 121–131. doi:10.1007/s00158-003-0318-3

[10] Honarmandi, P., Zu, J., and Behdinan, K., "Reliability-Based Design Optimization of Cantilever Beams Under Fatigue Constraint," *AIAA Journal*, Vol. 45, No. 11, 2007, pp. 2737–2746. doi:10.2514/1.24807

[11] Clauer, A. H., Walters, C. T., and Frod, S. C., "The Effects of Laser Shock Peening on the Fatigue Properties of 2024-T3 Aluminum," *Lasers in Materials Processing*, Vol. 7, American Society of Metals International, Materials Park, OH, 1983, pp. 7–22.

[12] Peyre, P., Fabbro, R., Merrien, P., and Lieurade, H., "Laser Shock Processing of Aluminum Alloys. Application to High Cycle Fatigue Behavior," *Materials Science and Engineering A*, Vol. 210, No. 1/2, 1996, pp. 102–113. doi:10.1016/0921-5093(95)10084-9

[13] Hatamleh, O., Lyons, J., and Forman, R., "Laser and Shot Peening Effects on Fatigue Crack Growth in Friction Stir Welded 7075-T7351 Aluminum Alloy Joints," *International Journal of Fatigue*, Vol. 29, No. 3, 2007, pp. 421–434. doi:10.1016/j.ijfatigue.2006.05.007

[14] Johnson, W., "Parametric Two-Dimensional Finite Element Investigation: Shot Peening of High-Strength Steel," *AIAA Journal*, Vol. 44,

No. 9, 2006, pp. 1973–1982.
doi:10.2514/1.19411

[15] Braisted, W., and Brockman, R., "Finite Element Simulation of Laser Shock Peening," *International Journal of Fatigue*, Vol. 21, No. 7, 1999, pp. 719–724.
doi:10.1016/S0142-1123(99)00035-3

[16] Wu, B., and Shin, Y. C., "From Incident Laser Pulse to Residual Stress: A Complete and Self-Closed Model for Laser Shock Peening," *Journal of Manufacturing Science and Engineering*, Vol. 129, No. 1, 2007, pp. 117–125.
doi:10.1115/1.2386180

[17] Ding, K., and Ye, L., "Three Dimensional Dynamic Finite Element Analysis of Multiple Laser Shock Peening Processes," *Surface Engineering*, Vol. 19, No. 5, 2003, pp. 351–358.
doi:10.1179/026708403225007563

[18] Singh, G., Grandhi, R. V., and Stargel, D. S., "Modeling and Parameter Design of a Laser Shock Peening Process," *International Journal for Computational Methods in Engineering Science & Mechanics* (to be published).

[19] Singh, G., Grandhi, R. V., Stargel, D. S., and Langer, K., "Modeling and Optimization of a Laser Shock Peening Process," AIAA Paper 2008-5838, Sept. 2008.

[20] Warren, A. W., Guo, Y. B., and Chen, S. C., "Massive Parallel Laser Shock Peening: Simulation, Analysis and Validation," *International Journal of Fatigue*, Vol. 30, No. 1, 2008, pp. 188–197.
doi:10.1016/j.ijfatigue.2007.01.033

E. Livne
Associate Editor